



Contents lists available at ScienceDirect

Tetrahedron

journal homepage: www.elsevier.com/locate/tet

Mesogenic heterocycles formed by bis-pyrazoles and bis-1,3,4-oxadiazoles

Kuan-Ting Lin, Gene-Hsiang Lee[†], Chung K. Lai^{*}

Department of Chemistry, National Central University, Chung-Li, Taiwan, ROC

ARTICLE INFO

Article history:

Received 1 March 2015

Received in revised form 14 April 2015

Accepted 18 April 2015

Available online xxx

Keywords:

Heterocycles

Bis-pyrazoles

Bis-1,3,4-oxadiazoles

Columnar

Catenar

ABSTRACT

Three new series of compounds **1a–c** containing multiple heterocyclic 2,5-pyrazoles, 1,3,4-oxadiazole and thiophene exhibiting mesophases were reported. Crystallographic data showed that the crystal **1a** ($n=8$) is a linear-shaped molecule with a molecular length of ca. 40.57 Å. However, three heterocyclic rings were not coplanar. All compounds **1a** formed smectic A/C phases, and all compounds **1c** exhibited columnar phases, which were confirmed by powder X-ray diffractometer (XRD). A N_{cell} and R_{ar} value equal to 3.91 and 18.29 Å within a slice of 9.0 Å thick were obtained for derivatives **1c** ($n=8$), indicating that two molecule was correlated within columns in Col_h phases. All derivatives showed good stabilities at temperature below $T=383\text{--}426$ °C on thermogravimetric analysis (TGA). The PL spectra of all compounds **1b–c** ($n=8$) showed one intense peak at $\lambda_{\text{max}}=428\text{--}496$ nm, and these photoluminescent emissions (PL) originated from 1,3,4-oxadiazole moiety.

© 2015 Elsevier Ltd. All rights reserved.

1. Introduction

Recently, a variety of heterocyclic derivatives have been applied to generate numerous organic electronic materials; these include semiconductors with high carrier mobilities, light-emitting diodes,¹ solar cells,² field-effect transistors,³ and others. Heteroatoms, such as nitrogen, oxygen, sulfur atoms incorporated into these heterocyclic moieties, might impact some chemical or physical properties, often not observed in their homologues all-carbon rings. All these heteroatoms are more electronegative than carbons, and they all have delocalized lone electrons. Mesogenic pyrazoles,⁴ 1,3,4-oxadiazoles,⁵ and thiophenes⁶ considered as a few of the most stable heterocyclic structures have been investigated in this group and others during past years. Their inherent features, such as electron unsaturation, electron-deficiency, nonplanar core or lower symmetries, higher polarizabilities and others were often responsible for their induction or formation of the mesophases. Pyrazoles are particularly interested due to their capabilities and abilities of forming H-bonds with neighboring molecules ($-\text{NH}\cdots\text{N}$). H-Bonds, though relatively weak in strength could be crucial, when a delicate balance between intermolecular interactions is needed to induce the mesophases. In contrast, it is well-known that 2,5-diary-1,3,4-oxadiazoles derivatives (OXD) showed high photoluminescence

quantum yields and good thermal and chemical stabilities. Many studies have demonstrated their widespread uses as electron-transporting/hole blocking materials, emitting layers in electroluminescent diodes or for non-linear optical processes.

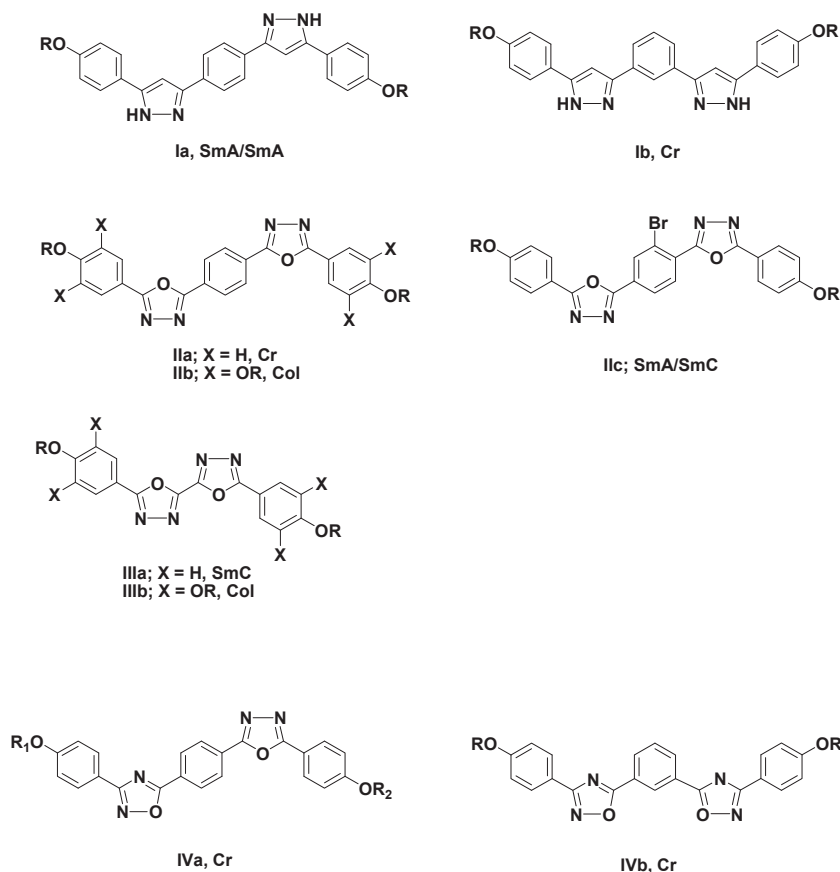
The effect of larger exocyclic angles caused by these heterocycles was also crucial in determine the overall shapes needed to induce the mesophases; $\epsilon \sim 151^\circ$, $\sim 149^\circ$ and $\sim 134^\circ$ for 2,5-pyrazoles, 2,5-thiophene, and 1,3,4-oxadiazoles, respectively. In general, the more linear structures were favorable to the appearance of mesophases. A few similar structures (see Scheme 1) of heterocyclic bis-pyrazoles **I**⁷ and bis-1,3,4-oxadiazoles **II**^{8–III}⁹ and **IV**¹⁰ were prepared and studied. Interestingly, crystallographic data of mesogenic compound **1a** ($n=14$) and non-mesogenic **1b** ($n=8$) indicated that an extended H-bonded structure was formed in both crystal lattices, giving a pseudo 1D-polymeric tape-like structure. Derivatives **1a** exhibited smectic A/C mesophases, in contrast, derivatives **1b** were all nonmesogenic. The difference in mesomorphic behavior was attributed to the between linear conformation and the coplanarity of the five rings over than in **1a**. Compound **11a** formed crystal phases. Compounds **11b**, classified as hexacatenar-shaped liquid crystals (LCs) exhibited columnar phases, and a strong blue light emission ($\lambda_{\text{max}} \sim 456$ nm) was observed with a higher quantum yields in dilute chloroform solution. A polar bromo group incorporated in compound **11c**^{8c} led to an asymmetric structure and greatly enhanced the formation of smectic phases. The twin-tapered bis-1,3,4-oxadiazole derivatives **111a** formed smectic phases. In contrast, compounds **111b** formed a layer-structured lyotropic LC and further formed a helical fibrous organo

^{*} Corresponding author. Tel.: +886 03 4259207; fax: +886 03 4277972; e-mail address: cklai@cc.ncu.edu.tw (C.K. Lai).

[†] Instrumentation Center, National Taiwan University, Taipei 10660, Taiwan, ROC.

<http://dx.doi.org/10.1016/j.tet.2015.04.055>

0040-4020/© 2015 Elsevier Ltd. All rights reserved.



Scheme 1. Examples of known bis-heterocyclic structures I–IV.

gel in DMF at concentrations above 0.6 wt%. The self-assembly process of **IIIb** in DMF was accompanied by a change in its fluorescence. The pitches of the helical fibers are non-uniform, and both left- and right-handed helical fibers are observed in equal quantities. Intermolecular π – π interactions between aromatic segments have been demonstrated to be the driving force for aggregate formation. A few star-shaped derivatives¹¹ made by tris-1,3,4-oxadiazoles exhibiting hexagonal columnar phases were also known. However, mesogenic bis-1,2,4-oxadiazoles¹² were relatively rare; compounds **IV** derived from 1,4-benzene or 1,3-benzene were not mesogenic.¹⁰

Here we wish to report the preparation, characterization, and mesomorphic studies of three series of heterocyclic bis-pyrazoles **1a** and bis-1,3,4-oxadiazoles **1b–c**. The mesogenic examples⁶ derived from thiophenes were relatively rare. The central core of 5-membered thiophene was incorporated to study the effect of mesomorphic behavior exhibited by other all-carbon 6-membered rings. An exocyclic angle^{6a} of 149.2° and 130.3°, respectively, for 2,5-thiophene and 1,3-benzene of bent-core mesogens was obtained by high-resolution solid state ¹³C NMR studies. All bis-pyrazoles **1a** were mesogenic, giving smectic A or/and smectic C phases. All compounds **1c** with six alkoxy chains exhibited hexagonal columnar phases, whereas, all compounds **1b** formed glass states. All bis-pyrazoles **1a** have a relatively high clearing temperature. Their optical properties are also discussed.

2. Results and discussions

2.1. Synthesis and characterization

The synthetic routes used to prepare bis-pyrazoles **1a** and bis-1,3,4-oxadiazoles **1b–c** are listed in Scheme 2. The yellow bis-

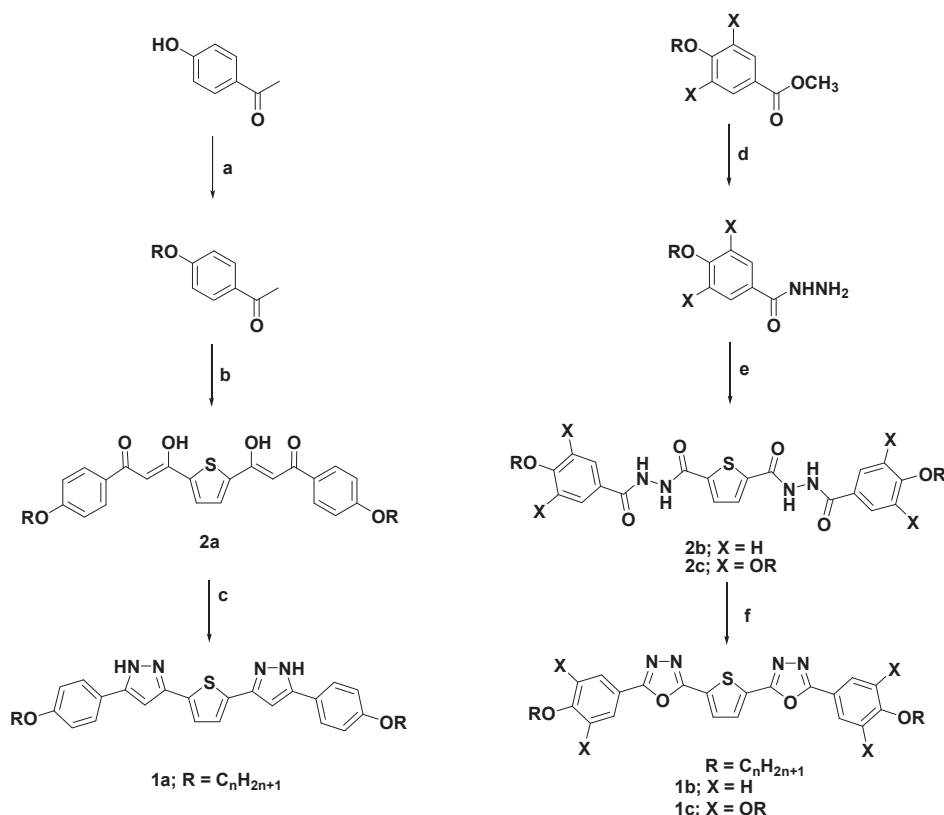
diketones **2a** were synthesized by double condensation of dimethyl thiophene-2,5-dicarboxylate, 1-(4-(octyloxy)phenyl)ethanone and NaH in refluxing dry THF for 6 h under nitrogen atmosphere. The yields were ranged from 55 to 60%. On ¹H NMR spectra, two singlet peaks appeared at δ 6.67 and δ 7.96 ppm is characteristically assigned for olefinic–H (–COH=CH) and thiophene–H. The bis-pyrazoles **1a**, isolated as white solids were obtained by the reactions of bis-diketones **2a** with excess hydrazine monohydrate in refluxing THF/methanol. The solubility of all bis-pyrazoles **1a** were poor in THF or chloroform at room temperature, therefore, most of final pyrazoles were only characterized by element analysis.

The formation of final pyrazoles was confirmed by a characteristic peak appeared at δ 12.22 ppm assigned to the pyrazole–H (–NH=C). The peak of thiophene–H was also shifted to δ 7.27 ppm.

On the other hand, bis-1,3,4-oxadiazoles **1b** were prepared by condensation reactions of N'2, N'5-bis(4-(alkoxy)benzoyl)thiophene-2,5-dicarbohydrazides **2b** was refluxed in phosphoryl chloride for 24 h. The final compounds **1b**, isolated as bright white-green solids were obtained after recrystallization from DCM/MeOH. Compounds **1b** were all characterized by either ¹H or ¹³C NMR spectroscopy in CDCl₃. On ¹³C NMR spectra, the observation of peaks occurred, for example, at 162.27 and 164.60 ppm, and also at 164.8 ppm was indicative of the formation of compounds **1b** ($n=8$) and **1c** ($n=8$), respectively.

2.2. Single crystal and molecular structures of 2,5-bis(5-(4-(octyloxy)phenyl)-1H-pyrazol-3-yl)thiophene **1a** ($n=8$)

In order to understand the correlation between the molecular structure and mesomorphic behavior, a single crystal of the



Scheme 2. Reactions and reagents. (a) RBr, K₂CO₃ and KI, refluxing in dry acetone, 24 h, 91–95%; (b) NaH, dimethyl thiophene-2,5-dicarboxylate, refluxing in dry THF, 6 h, 55–60%; (c) hydrazine monohydrate, acetic acid, refluxing in THF, MeOH, 24 h, 83%; (d) hydrazine monohydrate, refluxing in EtOH, 48 h, 65–70%; (e) thiophene-2,5-dicarboxylic acid and SOCl₂, refluxing in dry THF, 2 h; then, triethylamine, stirring in dry THF at rt, 24 h, 82–86%; (f) refluxing in POCl₃, 24 h, 78%.

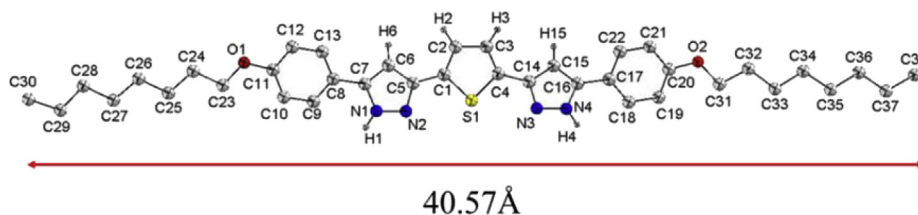


Fig. 1. An ORTEP plot for compound **1a** ($n=8$). The thermal ellipsoids of the non-hydrogen atoms are drawn at the 50% probability level.

mesogenic compound **1a** ($n=8$) suitable for crystallographic analysis was obtained by slow vaporization from THF at room temperature and its structure resolved. **Fig. 1** shows its molecular structure with the atomic numbering schemes. **Table 1** lists its crystallographic and structural refinement data for the crystal. It crystallizes in a triclinic space group P-1 with a $Z=2$. The overall molecular shape of the crystal **1a** ($n=8$) was considered as a linear-shaped, and the molecular length was ca. 40.57 Å (C38–C30). However, three heterocyclic rings were not coplanar; a total of dihedral angles; $\sim 26.52^\circ$ between the two pyrazolyl rings were obtained. The cause for the noncoplanarity might be attributed to the intermolecular interactions observed in the unit cell. Three H-bonds were formed. Two weak H-bonds between atoms N2–H1 ($d \sim 2.18$ Å) and atoms O2–H3 ($d \sim 2.82$ Å) were observed on the same layer. The other H-bond is formed between intermolecular pyrazole N3–H4 ($d \sim 2.17$ Å). All molecules were arranged by these three H-bonds to lead to a pseudo polymeric supramolecular structure. All three H-bonds were quite weak, whereas they were very important interaction in forming enantiotropic mesomorphism in this type of pyrazolyl structure. Such interaction might be induced by an interaction between the two electron-

withdrawing nitrogen atoms (δ^- -N) in central ring and δ^+ -H. A summary of intermolecular H-bonded interactions observed in **1a** ($n=8$) were listed in **Table 2**. All molecules were tilt arranged in the unit cell (**Fig. 3**).

2.3. Mesomorphic properties and thermal stabilities

The thermal behavior of compounds **1a–c** was investigated by polarized optical microscopy (POM) and differential scanning calorimetry (DSC). The transition temperatures and enthalpies of the compounds are listed in **Table 3**. All compounds **1a** and **1c** are mesogenic, whereas, all compounds **1b** were not mesogenic. All compounds **1a** exhibited smectic A or/and smectic C phases, which were all kinetically stable enantiotropic. Most of reported mesogenic pyrazolyl derivatives showed higher clearing temperatures than other similar heterocyclic derivatives, such as isozazoles or 1,3,4-oxdiazoles. For example, mesogenic 1,4-bis(5-(4-(octyloxy)phenyl)-1H-pyrazol-3-yl)benzene has a higher clearing temperature at $T_{Cl}=374.5^\circ\text{C}$. This series of compounds **1a** was no exception. The relatively higher clearing temperatures were often attributed to the capabilities and abilities of forming H-bonds with

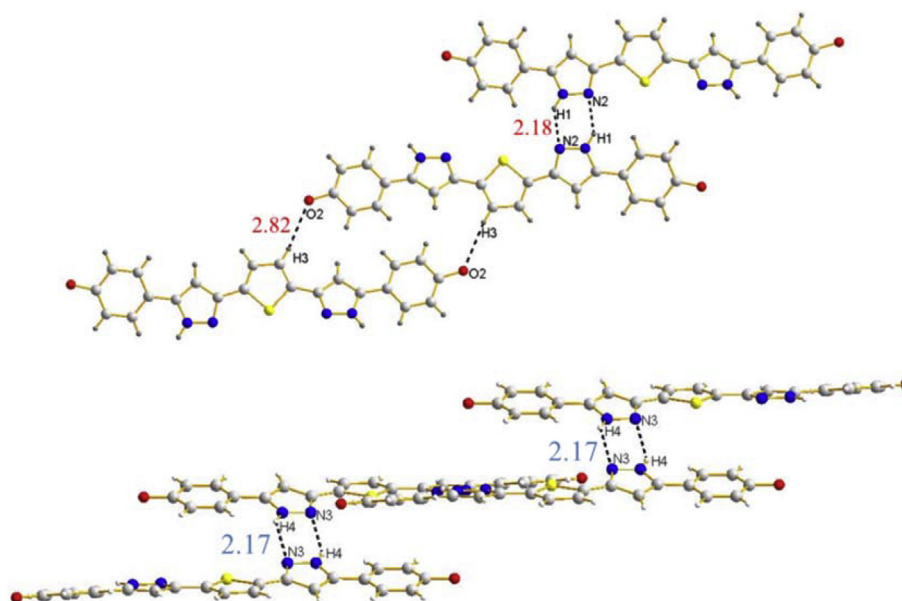


Fig. 2. The correlated structures induced by intermolecular H-bonds observed viewed from different axes in **1a** ($n=8$). Top plot: $H3\cdots O2=2.82$ Å, $H1\cdots N2=2.18$ Å; bottom: $H4\cdots N3=2.17$ Å.

Table 1

Crystallographic and experimental data for crystal **1a** ($n=8$)

Compd	1a ($n=8$)
Empirical formula	$C_{38}H_{48}N_4O_2S$
Formula weight	624.86
T/K	200(2)
Crystal system	Triclinic
Space group	P-1
$a/\text{Å}$	11.5430(11)
$b/\text{Å}$	11.5688(11)
$c/\text{Å}$	14.8260(15)
$\alpha/^\circ$	71.586(2)
$\beta/^\circ$	68.200(2)
$\gamma/^\circ$	89.975(2)
$U/\text{Å}^3$	1728.7(3)
Z	2
$F(000)$	672
$D_c/\text{mg m}^{-3}$	1.200
Crystal size/ mm^3	0.32 \times 0.12 \times 0.10
Range for data collection/ $^\circ$	1.57 to 25.00
Reflection collected	18,614
Data, restraints, parameters	6098, 4, 414
Independent reflection	6098 [$R(\text{int})=0.0647$]
Final $R1$, $wR2$	0.0744, 0.1431

Table 2

A summary of intermolecular H-bond interactions observed in **1a** ($n=8$)

Intermolecular H-bonds	
No. of H-bonds (C–H \cdots N)	2
Bond distance, angles	$N2-H1=2.18$ Å, $\angle N1-H1-N2=137.86^\circ$ $N3-H4=2.17$ Å, $\angle N3-H4-N4=131.11^\circ$
No. of H-bonds (C–H \cdots O)	1
Bond distance, angle	$O2-H3=2.82$ Å, $\angle O2-H3-C3=154.41^\circ$

neighboring molecules, as confirmed by single crystal structural analysis discussed above. Both melting and clearing temperatures were relatively high, and both crystallization temperatures and clearing temperatures of compounds **1a** decreased with carbon lengths of alkoxy chains. The melting temperatures were ranged

between $T_m=295.5$ °C ($n=8$) – 260.7 °C ($n=16$), while clearing temperatures were ranged between $T_{cl}=346.0$ °C ($n=8$) – 301.0 °C ($n=16$). On the other hands, the temperature range of mesophase remained at $\Delta T_M=41.1$ –52.7 °C during the cooling process. Under optical microscope, compounds **1a** ($n=8$) exhibited fan-shaped textures at higher temperatures and Schlieren textures at lower temperatures (Fig. 4). These two textures were characteristic of a layer smectic A and C phase expected for the rod-like molecules. Under optical microscope, a large area of homeotropic domains was also observed for SmA phase (Fig. 5).

Interestingly, all compounds **1b** were in fact nonmesogenic and two phase transitions of glass-to-isotropic occurred at $T_{cl}=244.1$ °C ($n=8$) and 230.4 °C ($n=12$) were observed. They formed glass states upon cooling from their isotropic states. Both series of compounds are structurally similar and the lack of H-bonds by **1b** needed to induce their mesophases was probably the main reason. Also, the clearing temperatures were much lower than those of compounds **1a** by 101.9–92.6 °C. In contrast, increasing the numbers of chains to six alkoxy in series of compounds **1c** led to the formation of columnar phase. These two compounds are not discotic in overall molecular shapes, but more catenar-shaped molecules. The formation of columnar phases formed by tetra-catenar or hexa-catenar heterocyclic derivatives was also known and reported in this group and others. All clearing temperatures were dramatically lowered to $T_{cl}=69.3$ –76.9 °C. However, the temperature range of columnar phases were ranged from $\Delta T_{CoI}=73.3$ ($n=12$)>44.7 ($n=8$) on the cooling process (Fig. 2). An optical texture, described as focal-conic texture with linear birefringent defects when slowly cooled from their isotropic liquids was observed, as shown in Fig. 4. The mesophases of both compounds **1c** ($n=8$) was identified by powder XRD experiments as hexagonal columnar phase.

The thermal stability of compounds **1a–c** ($n=8$) and **2a** ($n=8$) was also performed by thermogravimetric analyses (TGA) under nitrogen atmosphere, shown in Fig. 6. All four compounds showed good thermal stability at temperature below ca. 360.0 °C, with a relative thermal stability of **1a**>**1c**>**1b**>**2a**. The decomposition temperatures for a 5% weight loss were listed in Table 4. The decomposition temperature of **1a** is much higher than that of **1b** by ca. $\Delta T=43.4$ °C, which is quite consistent with the DSC data of these

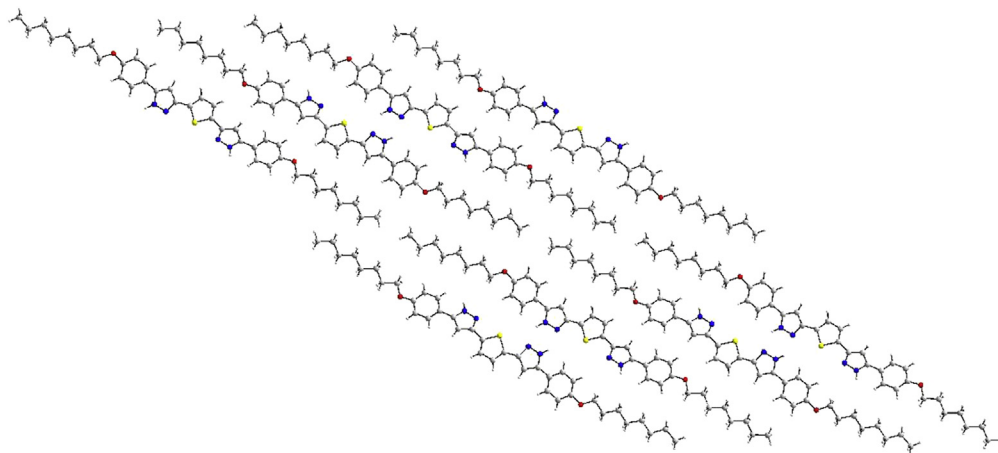


Fig. 3. The molecular arrangements in the unit cell by **1a** ($n=8$).

Table 3
The phase transitions and enthalpies^a of compounds **1a–1c**

1a; $n=8$	Cr	<u>295.5 (33.0)</u>	SmC	<u>340.4 (1.01)</u>	SmA	<u>346.0 (10.1)</u>	I
		292.0 (30.8)		<u>340.0 (2.30)</u>		<u>344.7 (9.25)</u>	
$n=10$	Cr	<u>284.8 (34.6)</u>	SmC	<u>333.3 (12.9)</u>	SmC	<u>330.4 (6.66)</u>	I
		281.2 (26.0)		<u>323.0 (10.2)</u>		<u>322.2 (8.07)</u>	
$n=12$	Cr	<u>275.1 (25.4)</u>	SmC	<u>309.8 (8.99)</u>	SmC	<u>305.0 (6.15)</u>	I
		272.2 (23.6)		<u>301.0 (10.7)</u>		<u>300.5 (10.2)</u>	
$n=14$	Cr	<u>268.0 (21.9)</u>	SmC	<u>244.1 (32.5)</u>	G	<u>236.9 (32.3)</u>	I
		263.9 (20.1)		<u>230.4 (39.0)</u>		<u>226.3 (39.0)</u>	
$n=16$	Cr	<u>260.7(30.7)</u>	SmC	<u>244.1 (32.5)</u>	G	<u>230.4 (39.0)</u>	I
		258.0 (28.8)		<u>226.3 (39.0)</u>		<u>226.3 (39.0)</u>	
1b; $n=8$					G	<u>244.1 (32.5)</u>	I
						<u>230.4 (39.0)</u>	
$n=12$					G	<u>230.4 (39.0)</u>	I
						<u>226.3 (39.0)</u>	
1c; $n=8$	Cr	<u>45.9 (20.8)</u>	Col	<u>69.3 (1.79)</u>	Col	<u>66.4 (1.80)</u>	I
		21.7 (10.0)		<u>76.9 (3.36)</u>		<u>75.3 (3.19)</u>	
$n=12$	Cr	<u>57.3 (90.3)</u>	Col	<u>76.9 (3.36)</u>	Col	<u>75.3 (3.19)</u>	I
		2.0 (12.3)		<u>75.3 (3.19)</u>		<u>75.3 (3.19)</u>	

^a: n = the carbon numbers of alkoxy chains; Cr = crystal; G = glass, SmA = smectic A, SmC = smectic C, Col = columnar, I = isotropic phases measured at a scan rate of 10⁰C/min.

two compounds. The clearing temperature of compound **1a** ($n=8$) is higher than that of compound **1b** ($n=8$) by $\Delta T_{cl}=101.9$ °C.

2.4. Powder X-ray diffractions and packing arrangements

Variable-temperature powder XRD diffraction experiments were performed to confirm the structure of the mesophases of compounds **1a** ($n=14$) and **1c** ($n=8$), and a summary of diffraction data was listed in Table 5. For example, for compounds **1a** ($n=14$) at 265 °C a diffraction pattern with one strong peak at 39.22 Å and one very weak peak at 19.81 Å at small angle region, was observed, as shown in Fig. 7. These two diffraction peaks at lower angle were assigned as 001 and 002, which were typically characteristics of layer structures observed for a SmC phase. A layer d -spacing of 39.22 Å, compared to 58.0 Å obtained for the molecular length of the dimeric structure calculated by MM2 indicated that all molecules were possibly tilt or/and the alkoxy carbon chains were interdigitated. A broad halo peak appeared at 4.80 Å was also

observed for this compound, as shown in Fig. 7. In contrast, compounds **1c** formed columnar phases. On XRD plot, a typical diffraction pattern of a two-dimensional hexagonal lattice with one very strong diffraction peak at lower angle and three much weaker diffraction peaks of compound **1c** ($n=8$) was obtained at 65.0 °C under cooling process, shown in Fig. 7. A diffraction pattern with a d -spacing at 27.13, 15.97, and 13.89 Å, and a broad diffuse peak 4.35 Å at wide-angle region was obtained. This diffraction pattern corresponded to a hexagonal columnar arrangement with a d -spacing ratio of 1, $(1/3)^{1/2}$, and $(1/4)^{1/2}$, corresponding to Miller indices: 100, 110 and 200, respectively. This diffraction pattern corresponded to an intercolumnar distance or lattice constant (*i.e.*, a parameter of the hexagonal lattice) of 31.33 Å. The lack of any relatively peaks at wide angles excluded a more regular periodicity along the columns. However, liquid-like correlations between the rigid cores occurred at wide angle regions of 4.35 Å.

Both values of N_{cell} and R_{ar} were also obtained from lattice parameters of X-ray diffraction as shown in Table 6. These two values



Fig. 4. Optical textures of observed by compounds: SmA phase by **1a** ($n=8$, top left) at 344 °C; SmC phase by **1a** ($n=8$, top right) at 335 °C; columnar phase by **1c** ($n=8$, bottom left) at 60 °C and columnar phase by **1c** ($n=12$, bottom right) at 63 °C.

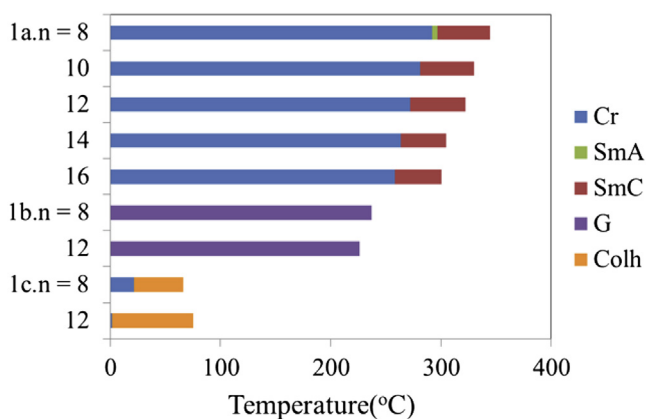


Fig. 5. Bar graphs showing the phase behavior of compounds **1a–c**. All temperatures were taken on the cooling process.

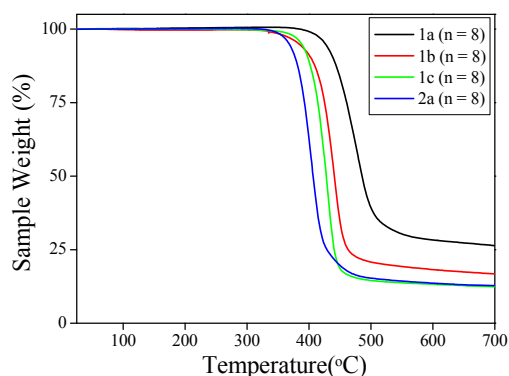


Fig. 6. The TGA thermographs of compounds **1a–c** and **2a** (all $n=8$) under nitrogen gas at a heating rate of 10.0 °C min⁻¹.

Table 4

The decomposition temperatures^a of compounds **1a–c** and **2a** by TGA analysis

Compds	T_{dec} (°C)
1a ($n=8$)	426.7
1b ($n=8$)	383.3
1c ($n=8$)	387.5
2a ($n=8$)	367.5

^a Temperatures taken with a 5% weight loss under nitrogen atmosphere.

Table 5

Detailed indexing by powder XRD diffraction for compounds **1a**, **1c**

Compd	Mesophases temp ^a	d -Spacing obs. (calcd)	Lattice const. (Å)	Miller indices
1a ($n=14$)	SmC at 260.0 °C	39.22 (39.22)	$a=31.33$	001
		19.81 (19.61)		002
		4.80 (br)		Halo
1c ($n=8$)	Col at 65 °C	27.13 (27.63)	$a=31.33$	100
		15.97 (15.94)		110
		13.89 (13.81)		200
		4.35 (br)		Halo

^a Temperature taken on the cooling process.

were useful to understand the possible molecular packing in the columnar phases. The detail calculations were not discussed here. A value of $N_{cell}=3.91$ was obtained for compounds **1c** ($n=8$) within a height of 9.0 Å in the columnar phase. The overall molecular shapes of compounds **1c** were more catenar-shaped. Therefore, a more disc-like correlated structure constructed by two molecules lying side-by-side was generated within the column. The possible molecular arrangement in columnar phases was proposed in Fig. 8.

2.5. Optical properties

The UV–vis absorption and PL spectra of the compounds **1a–c** (all $n=8$) measured in CH₂Cl₂ solution at room temperature are presented in Fig. 9 and data presented in Table 7. These compounds containing three adjacent heterocyclic moieties are particularly

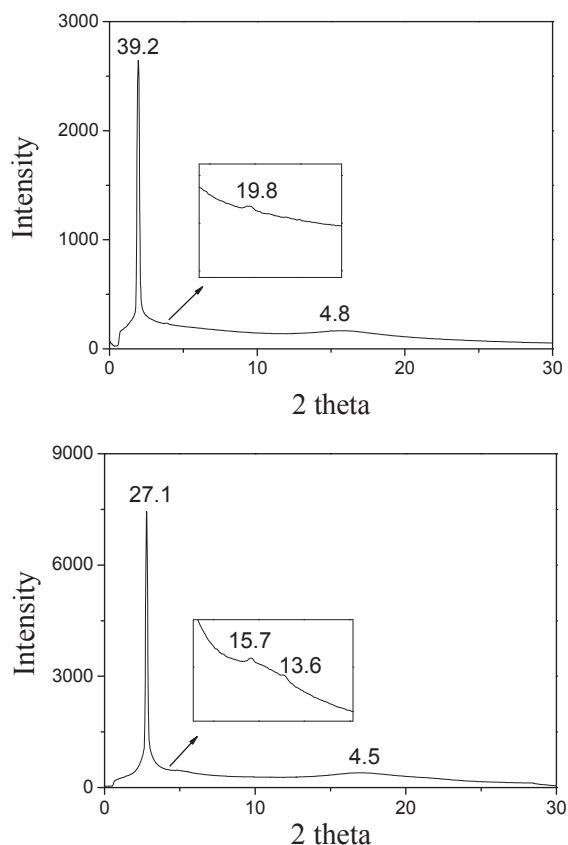


Fig. 7. Powder X-ray diffraction plots of compounds: **1a** ($n=14$; top plot) at 260.0 °C and **1c** ($n=8$; bottom plot) at 65.0 °C when cooled from above their clearing temperatures.

Table 6
Geometric parameters^a of compound **1c** ($n=8$)

Compd	S (Å ²)	V_{cell} (Å ³)	V_m (Å ³)	Temp (°C)	N_{cell}	S_{ar} (Å ²)	R_{ar} (Å)
1c ($n=8$)	849.90	7649.12	1955.39	65.0	3.91	262.61	18.29

^a S (Å²)=columnar cross section area, V_{cell} (Å³)=volume of the column stratum 9 Å thick, V_m (Å³)=molecular volume, N_{cell} =the number of molecules contained in each columnar stratum 9-Å thick, S_{ar} (Å²)=the surface area of hard columnar core, R_{ar} (Å)=the diameter of the aromatic part.

interesting due to the presence of multiple chromophores and possible π -conjugations between the peripheral structures and central core. The λ_{max} peaks of UV-vis absorption and the λ_{max} of PL spectra were listed in Table 7. The absorption λ_{max} peaks of compounds **1a–c** occurred at ca. 303–365 nm, which were attributed to π - π^* transitions arising from the pyrazoles and oxadiazole.¹³ In contrast, absorption λ_{max} peaks at ca. 261–275 nm were attributed to the π - π^* transitions arising from the thiophene. The λ_{max} for compound **1a** occurred at 380 nm, and its intensity was relatively weak. The PL spectra of all compounds **1b–c** showed one intense and broad peak occurred at λ_{max} =428 and 496 nm, respectively, and these photoluminescent emission originated from heterocyclic bis-pyrazoles **1a** and bis-1,3,4-oxadiazoles **1b–c**. Compounds **1b–c** are potentially better blue-emitters. In general, a red-shift emission is often expected in this type of conjugated systems. However, the two λ_{max} peaks observed by bis-oxadiazoles **1b–c** were much different from those of other similar mono-1,3,4-oxadiazoles. Central thiophene is often considered as a more electron-donating group; λ_{max} for compounds **1b** and **1c** was slightly red shifted by ca. ~31 and ~40 nm when compared with the similar all-carbon

compounds **1a** and **1c**, respectively. An apparent red-shift of ca. ~68 nm by compound **1c** over **1b** was also observed, which might be attributed to the more electron-donating group of six alkoxy chains in **1c**. All quantum yields of luminescent materials were ranged from 14 to 25%.

3. Conclusions

Three new series of bis-pyrazoles **1a** and bis-1,3,4-oxadiazoles **1b–c** were prepared and studied; all compounds **1a** formed smectic A and/or C phases, and other compounds **1c** exhibited hexagonal columnar phases. Compounds **1a** exhibited an improved mesomorphic behavior than other similar bis-pyrazoles **1b**, which might be attributed to the larger exocyclic angle by central 2,5-thiophene ($\epsilon \sim 149^\circ$) than homologues replaced by 1,3-benzene ($\epsilon \sim 120^\circ$) in **1b**. An apparent red-shift in PL wavelength by such bis-1,3,4-oxadiazoles **1b–c** compared to other similar mono-1,3,4-oxadiazoles due to their conjugated structures.

4. Experimental section

4.1. General materials and methods

All chemicals and solvents were reagent grade from Aldrich Chemical Co., and solvents were dried by standard techniques. ¹H and ¹³C NMR spectra were measured on a Bruker DRS-300. DSC thermographs were carried out on a Mettler DSC-822 and calibrated with a pure indium sample. All phase transitions are determined by a scan rate of 10.0 °C/min. Optical polarized microscopy was carried out on Zeiss Axioplan 2 equipped with a hot stage system of Mettler FP90/FP82HT. The UV-vis absorption and fluorescence spectra were obtained using a Jasco V-530 and Hitachi F-4500 spectrometer. All spectra were measured in CH₂Cl₂ at room temperature, and the excitation wavelengths of the fluorescent spectra were 303 nm (for **1a**), 354 nm (for **1b**) and 365 nm (for **1c**). Elemental analyses were performed on a Heraeus CHN-O-Rapid elemental analyzer. The powder diffraction data were collected from the Wiggler-A beam line of the National Synchrotron Radiation Research Center (NSRRC) with a wavelength of 1.3223 Å. The powder samples were charged in Lindemann capillary tubes (80 mm long and 0.01 mm thick) from Charles Supper Co. with an inner diameter of 1.0 mm.

4.2. Synthesis of the compounds 1a–c

4.2.1. 1-(4-(Octyloxy)phenyl)ethanone. ¹H NMR (300 MHz, CDCl₃): δ 0.82 (t, 3H, -CH₃, $J=6.9$ Hz), 1.21–1.77 (m, 10H, -CH₂), 1.74–1.84 (m, 2H, -CH₂), 2.50 (s, 3H, -CH₃), 3.97 (t, 2H, -OCH₂), 6.88 (d, Ar-H, 2H, $J=8.7$ Hz), 7.89 (d, Ar-H, 2H, $J=8.7$ Hz). ¹³C NMR (75 MHz, CDCl₃): δ 13.99, 22.58, 25.87, 26.07, 29.02, 29.25, 29.45, 31.79, 68.10, 113.98, 129.98, 163.00, 196.30.

4.3. (2Z,2'Z)-3,3'-(Thiophene-2,5-diyl)bis(3-hydroxy-1-(4-(octyloxy)phenyl)prop-2-en-1-one) 2a (n=8)

The solution 1-(4-(octyloxy)phenyl)ethanone (1.0 g, 0.004 mol) and NaH (0.16 g, 0.012 mol) dissolved in 50 mL of dry THF heated to 40 °C for 30 min under nitrogen atmosphere. The solution turned deep red. Then dimethyl thiophene-2,5-dicarboxylate (0.41 g, 0.004 mol) was added and then the solution was refluxed for 6 h under nitrogen atmosphere. The solution was cooled and neutralized with aqueous 1.0 M hydrochloric acid. The solution was twice extracted with 100 mL of dichloromethane, and the organic layers were collected and dried. The product, isolated as yellow solids was obtained after recrystallization from THF/MeOH. Yield 60%.

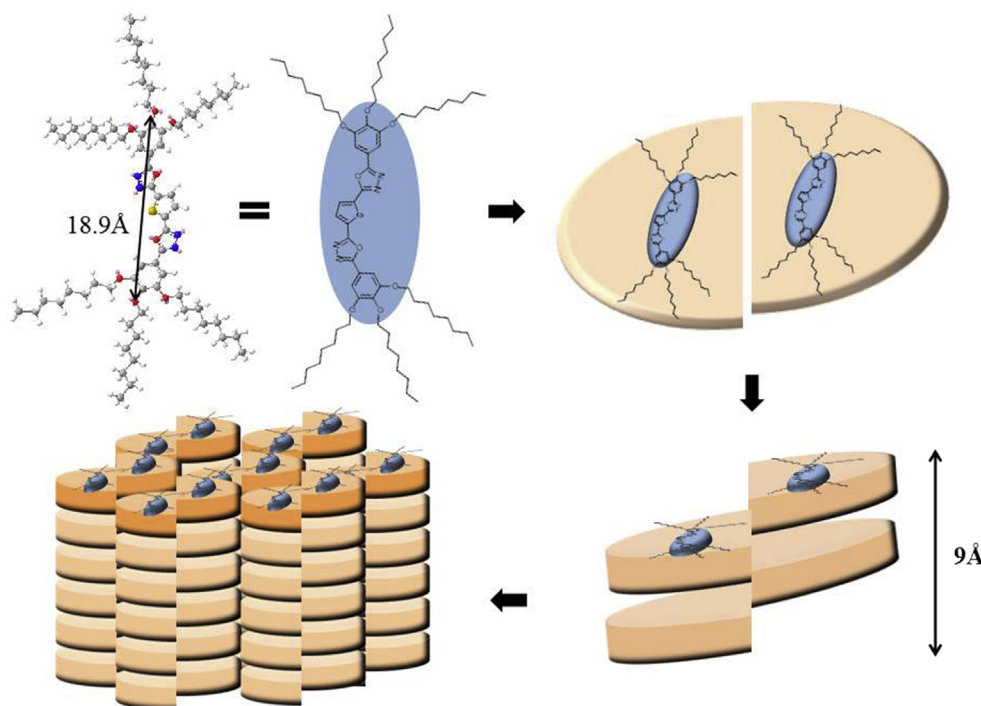


Fig. 8. A schematic representation of molecular organization proposed in columnar phase by compounds **1c** ($n=8$).

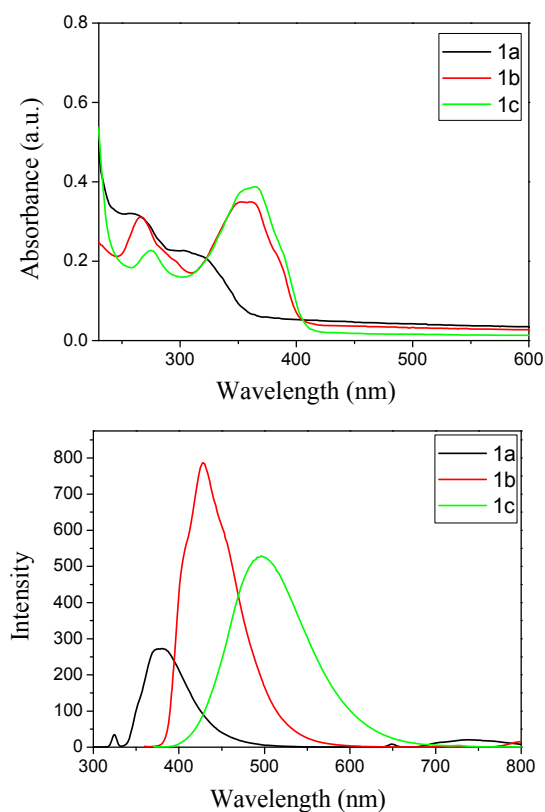


Fig. 9. Absorption (top), PL spectra (central) and PL normalized spectra (bottom) of the compounds **1a–c**.

$^1\text{H NMR}$ (300 MHz, CDCl_3): δ 0.87–0.92 (m, 6H, $-\text{CH}_3$), 1.31–1.51 (m, 20H, $-\text{CH}_2$), 1.77–1.83 (m, 4H, $-\text{CH}_2$), 4.06 (t, 4H, $-\text{OCH}_2$, $J=6.3$ Hz), 6.67 (s, 2H, $-\text{CH}=\text{C}$), 7.01 (d, 4H, Ar–H, $J=7.2$ Hz), 7.96 (s, 2H, thiophene–H), 8.03 (d, 4H, Ar–H, $J=7.2$ Hz). $^{13}\text{C NMR}$ (75 MHz,

Table 7

The UV–vis absorption and PL emission data^a of compound **1**

Compds	Absorption λ_{max} (nm)	Emission λ_{max} (nm)	Φ_{F}
1a ($n=8$)	261, 303	380	14.0
1b ($n=8$)	266, 354	428	25.2
1c ($n=8$)	275, 365	496	24.1
11a ($n=8$) ^{8d}	329, 339	397	
11b ($n=8$) ^{8b}	270, 340	456	
11c ($n=8$) ^{8c}	335	436	

^a Measured in CH_2Cl_2 solution (5.0×10^{-6} M) at rt. The standard is anthracene ($\Phi_{\text{F}}=0.27$ in hexane solution) and n is reflective indices of solvents; $n_{\text{CH}_2\text{Cl}_2}=1.42440$, $n_{\text{hexane}}=1.37506$. Also see Refs. **8b–d** for optical data of compounds **11a–c**.

CDCl_3): δ 14.60, 23.72, 24.96, 25.22, 25.49, 25.76, 26.02, 27.13, 30.30, 30.41, 30.50, 32.98, 69.18, 93.05, 115.44, 127.76, 130.27, 131.25, 147.91, 164.46, 180.99, 184.34.

4.3.1. 2,5-Bis(5-(4-(octyloxy)phenyl)-1H-pyrazol-3-yl)thiophene 1a ($n=8$). The solution of (2Z,2'Z)-3,3'-(thiophene-2,5-diyl)bis(3-hydroxy-1-(4-(octyloxy)phenyl)prop-2-en-1-one) (1.00 g, 2.0 mmol) dissolved in 50 mL THF was slowly added 0.5 mL of glacial acetic acid and the solution was stirred for 5 min. Then hydrazine (1.0 mL) was added and then refluxed for 24 h. The solution was concentrated to dryness. The product, isolated as white solid was obtained after recrystallization from THF/MeOH. Yield 83%, $^1\text{H NMR}$ (300 MHz, d-THF): δ 0.87–0.90 (m, 6H, $-\text{CH}_3$), 1.31–1.49 (m, 20H, $-\text{CH}_2$), 1.75–1.81 (m, 4H, $-\text{CH}_2$), 3.99 (t, 4H, $-\text{OCH}_2$, $J=6.3$ Hz), 6.74 (s, 2H, $-\text{CH}=\text{C}$), 6.95 (d, 4H, Ar–H, $J=8.4$ Hz), 7.27 (s, 2H, thiophene–H), 7.63 (d, 4H, Ar–H, $J=8.4$ Hz), 12.22 (s, 2H, $-\text{NH}=\text{C}$). Anal. Calcd for $\text{C}_{38}\text{H}_{48}\text{N}_4\text{O}_2\text{S}$: C, 73.04; H, 7.74. Found C, 72.95; H, 7.74. MS (HRFAB): calcd for M^+ : 624.3498. Found: 624.3502.

4.3.2. 2,5-Bis(5-(4-(decyloxy)phenyl)-1H-pyrazol-3-yl)thiophene 1a ($n=10$). NMR data are not available due to its poor solubility. Anal.

Calcd for $C_{42}H_{56}N_4O_2S$: C, 74.08; H, 8.29. Found C, 73.89; H, 8.28. MS (HRFAB): calcd for M^+ : 680.4124. Found: 680.4128.

4.3.3. *2,5-Bis(5-(4-(dodecyloxy)phenyl)-1H-pyrazol-3-yl)thiophene 1a* ($n=12$). NMR data are not available due to its poor solubility. Anal. Calcd for $C_{46}H_{64}N_4O_2S$: C, 74.96; H, 8.75. Found C, 74.85; H, 8.77. MS (HRFAB): calcd for M^+ : 736.4750. Found: 736.4745.

4.3.4. *2,5-Bis(5-(4-(tetradecyloxy)phenyl)-1H-pyrazol-3-yl)thiophene 1a* ($n=14$). NMR data are not available due to its poor solubility. Anal. Calcd for $C_{50}H_{72}N_4O_2S$: C, 75.71; H, 9.15. Found C, 75.41; H, 9.12. MS (HRFAB): calcd for M^+ : 792.5376. Found: 792.5377.

4.3.5. *2,5-Bis(5-(4-(hexadecyloxy)phenyl)-1H-pyrazol-3-yl)thiophene 1a* ($n=16$). NMR data are not available due to its poor solubility. Anal. Calcd for $C_{54}H_{80}N_4O_2S$: C, 76.37; H, 9.49. Found C, 76.25; H, 9.46.

4.4. 4-(Octyloxy)benzohydrazide

The solution of methyl-4-(dodecyloxy)benzoate (5.0 g, 0.02 mol) dissolved in 100 mL of MeOH was added hydrazine monohydrate (3.1 g, 0.2 mol). The solution was refluxed for 12 h. The solution was concentrated to give off-white solids. The products, isolated as white solids were obtained after recrystallization from hexane/MeOH. Yield 90%, 1H NMR (300 MHz, $CDCl_3$): δ 0.86 (t, 3H, $-CH_3$, $J=5.7$ Hz), 1.24–1.42 (m, 10H, $-CH_2$), 1.73–1.78 (m, 4H, $-CH_2$), 4.00 (t, 2H, $-OCH_2$, $J=6.3$ Hz), 6.87 (d, 2H, Ar–H, $J=8.4$ Hz), 7.69 (d, 1H, Ar–H, $J=8.4$ Hz), 7.77 (s, 1H, N–H). ^{13}C NMR (75 MHz, $CDCl_3$): δ 14.08, 22.65, 25.94, 29.07, 29.32, 29.54, 29.60, 31.87, 68.16, 114.34, 124.51, 128.63, 129.23, 162.05, 168.36.

4.5. N'2, N'5-Bis(4-(octyloxy)benzoyl)thiophene-2,5-dicarbohydrazide 2b ($n=8$)

The solution of thiophene-2,5-dicarboxylic acid (1.0 g, 6.0 mmol) and 2.0 mL of thionyl chloride (0.016 mol) was gently refluxed in dry THF for 4 h under nitrogen atmosphere. The excess of thionyl chloride was removed under reduced vacuum. The compound prepared was then used directly for the following step. The solution of 4-(octyloxy)benzohydrazide (3.2 g, 0.012 mol) dissolved in 60 mL of THF was dropwise added 0.14 mL of triethylamine (1.0 mmol) at ice bath. The solution was stirred at rt for 24 h. The solution was extracted twice with 100 mL of CH_2Cl_2/H_2O . The organic layers were combined and concentrated to give white solids. The products, isolated as white solids were obtained after recrystallization from THF/MeOH. Yield 83%, 1H NMR (300 MHz, $CDCl_3$): δ 0.86 (t, 6H, $-CH_3$, $J=6.3$ Hz), 1.27–1.42 (m, 20H, $-CH_2$), 1.70–1.75 (m, 4H, $-CH_2$), 4.04 (t, 4H, $-OCH_2$, $J=6$ Hz), 7.04 (d, 4H, Ar–H, $J=8.4$ Hz), 7.87 (d, 4H, Ar–H, $J=9$ Hz), 7.90 (s, 2H, thiophene–H), 10.4 (s, 2H, N–H), 10.7 (s, 2H, N–H). ^{13}C NMR (75 MHz, $CDCl_3$): δ 13.99, 22.11, 25.49, 28.58, 28.68, 28.74, 31.26, 67.77, 106.52, 114.23, 124.26, 129.41, 141.34, 160.33, 161.63, 165.41.

4.6. N'2, N'5-Bis(3,4,5-tris(octyloxy)benzoyl)thiophene-2,5-dicarbohydrazide 2c ($n=8$)

1H NMR (300 MHz, $CDCl_3$): δ 0.86 (t, 18H, $-CH_3$, $J=6.3$ Hz), 1.18–1.42 (m, 60H, $-CH_2$), 1.63–1.78 (m, 12H, $-CH_2$), 3.89–3.98 (m, 12H, $-OCH_2$), 7.51 (s, 2H, Ar–H), 7.60 (s, 2H, Ar–H), 7.92 (s, 2H, thiophene–H), 10.6 (s, 2H, N–H), 11.0 (s, 2H, N–H). ^{13}C NMR (75 MHz, $CDCl_3$): δ 14.07, 22.62, 22.67, 25.98, 26.07, 26.17, 29.16, 29.24, 29.29, 29.43, 29.53, 30.32, 31.72, 68.89, 69.05, 69.19, 69.38, 106.24, 114.23, 124.46, 125.58, 140.96, 158.23, 161.60, 166.61.

4.6.1. *2,5-Bis(5-(4-(octyloxy)phenyl)-1,3,4-oxadiazol-2-yl)thiophene 1b* ($n=8$). The solution of N'2, N'5-bis(4-(octyloxy)benzoyl)thiophene-2,5-dicarbohydrazide (1.0 g, 2.0 mmol) dissolved in 40 mL of phosphoryl chloride was refluxed for 24 h. The solution slowly turned reddish-black in color. The solution was cooled at room temperature, and then the solution was slowly poured into 300 mL of ice water. After stirring for 2 h, the orange-red solids were filtered and collected. The solids were dissolved in 25 mL of dichloromethane and extracted with 150 mL of 1.0 M $NaOH_{(aq)}$. The products, isolated as yellow-green solids were obtained after recrystallization from DCM/MeOH. Yield 80%, 1H NMR (300 MHz, $CDCl_3$): δ 0.87 (t, 6H, $-CH_3$, $J=6.9$ Hz), 1.27–1.46 (m, 20H, $-CH_2$), 1.75–1.82 (m, 4H, $-CH_2$), 4.01 (t, 4H, $-OCH_2$, $J=6.3$ Hz), 7.00 (d, 4H, Ar–H, $J=9$ Hz), 7.81 (s, 2H, thiophene–H), 8.02 (d, 4H, Ar–H, $J=9$ Hz). ^{13}C NMR (75 MHz, $CDCl_3$): δ 14.08, 22.64, 25.98, 29.10, 29.21, 29.32, 31.79, 68.10, 115.06, 115.45, 128.83, 129.71, 159.43, 162.27, 164.61. Anal. Calcd for $C_{36}H_{44}N_4O_4S$: C, 68.76; H, 7.05. Found C, 67.96; H, 7.01.

4.6.2. *2,5-Bis(5-(4-(dodecyloxy)phenyl)-1,3,4-oxadiazol-2-yl)thiophene 1b* ($n=12$). 1H NMR (300 MHz, $CDCl_3$): δ 0.86 (t, 6H, $-CH_3$, $J=6.9$ Hz), 1.25–1.46 (m, 36H, $-CH_2$), 1.78–1.81 (m, 4H, $-CH_2$), 4.03 (t, 4H, $-OCH_2$, $J=6.3$ Hz), 7.01 (d, Ar–H, 4H, $J=9$ Hz), 7.84 (s, 2H, thiophene–H), 8.04 (d, Ar–H, 4H, $J=9$ Hz). ^{13}C NMR (75 MHz, $CDCl_3$): δ 14.11, 22.68, 25.98, 29.10, 29.35, 29.63, 31.91, 68.33, 115.06, 115.44, 128.83, 129.71, 159.43, 162.27, 164.61. Anal. Calcd for $C_{44}H_{60}N_4O_4S$: C, 71.32; H, 8.16. Found C, 71.25; H, 8.16.

4.6.3. *2,5-Bis(5-(3,4,5-tris(octyloxy)phenyl)-1,3,4-oxadiazol-2-yl)thiophene 1c* ($n=8$). 1H NMR (300 MHz, $CDCl_3$): δ 0.87 (t, 18H, $-CH_3$, $J=6.9$ Hz), 1.23–1.49 (m, 60H, $-CH_2$), 1.76–1.86 (m, 12H, $-CH_2$), 4.01–4.10 (m, 12H, $-OCH_2$), 7.29 (s, 4H, Ar–H), 7.87 (s, 2H, thiophene–H). ^{13}C NMR (75 MHz, $CDCl_3$): δ 14.08, 22.66, 26.06, 29.34, 29.50, 30.33, 31.81, 31.88, 69.43, 73.65, 105.55, 117.79, 128.81, 129.89, 141.75, 153.66, 159.70, 164.80. Anal. Calcd for $C_{68}H_{108}N_4O_8S$: C, 71.54; H, 9.53. Found C, 71.61; H, 9.60.

4.6.4. *2,5-Bis(5-(3,4,5-tris(dodecyloxy)phenyl)-1,3,4-oxadiazol-2-yl)thiophene 1c* ($n=12$). 1H NMR (300 MHz, $CDCl_3$): δ 0.86 (t, 18H, $-CH_3$, $J=6.9$ Hz), 1.24–1.57 (m, 108H, $-CH_2$), 1.70–1.88 (m, 12H, $-CH_2$), 4.01–4.08 (m, 12H, $-OCH_2$), 7.29 (s, 4H, Ar–H), 7.87 (s, 2H, thiophene–H). ^{13}C NMR (75 MHz, $CDCl_3$): δ 14.10, 22.68, 26.07, 29.39, 29.64, 29.69, 30.34, 31.92, 69.42, 73.65, 105.54, 117.78, 128.82, 129.88, 141.75, 153.66, 159.70, 164.80. Anal. Calcd for $C_{92}H_{156}N_4O_8S$: C, 74.75; H, 10.64. Found C, 74.73; H, 10.61.

Acknowledgements

We thank the Ministry of Science and Technology, Taiwan, ROC (MOST 103-2113-M-008-002) for generous support of this work.

Supplementary data

Supplementary data related to this article can be found at <http://dx.doi.org/10.1016/j.tet.2015.04.055>.

References and notes

- (a) Kulkarni, A. P.; Tonzola, C. J.; Babel, A.; Jenekhe, S. A. *Chem. Mater.* **2004**, *16*, 4556–4573; (b) Oyston, S.; Wang, C.; Hughes, G.; Batsanov, A. S.; Perepichka, I. F.; Bryce, M. R.; Ahn, J. H.; Pearson, C.; Petty, M. C. *J. Mater. Chem.* **2005**, *15*, 194–203; (c) Ichikawa, M.; Kawaguchi, T.; Kobayashi, K.; Miki, T.; Furukawa, T.; Koyama, T.; Taniguchi, Y. *J. Mater. Chem.* **2006**, *16*, 221–225.
- (a) Mende, L. S.; Fechtenkotter, A.; Mullen, K.; Moons, E.; Friend, R. H.; MacKenzie, J. D. *Science* **2001**, *293*, 1119–1122; (b) Hesse, H. C.; Weickert, J.; Al-Hussein, M.; Dossel, L.; Feng, X.; Mullen, K.; Mende, L. S. *Sol. Energy Mater. Sol. Cells* **2010**, *94*, 560–567.
- Zhao, X.; Zhan, X. *Chem. Soc. Rev.* **2011**, *40*, 3728–3743.

4. (a) Cuerva, C.; Campo, J. A.; Ovejero, P.; Torres, M. R.; Oliveria, E.; Santos, S. M.; Lodeiro, C.; Cano, M. J. *Mater. Chem. C* **2014**, *2*, 9167–9181; (b) Cuerva, C.; Campo, J. A.; Ovejero, P.; Torres, M.; Cano, M. *Dalton Trans.* **2014**, *43*, 8849–8860; (c) Cuerva, C.; Ovejero, P.; Campo, J. A.; Cano, M. *Dalton Trans.* **2014**, *38*, 511–517; (d) Kuo, H. M.; Tsai, S. L.; Lee, G. H.; Sheu, H. S.; Lai, C. K. *Tetrahedron* **2013**, *69*, 618–626; (e) Chou, S. Y.; Chen, C. J.; Tsai, S. L.; Sheu, H. S.; Lee, G. H.; Lai, C. K. *Tetrahedron* **2009**, *65*, 1130–1139; (f) Chen, M. C.; Lee, S. C.; Ho, C. C.; Hu, T. S.; Lee, G. H.; Lai, C. K. *Tetrahedron* **2009**, *65*, 9460–9467.
5. (a) Lu, L. Y.; Kuo, H. M.; Sheu, H. S.; Lee, G. H.; Lai, C. K. *Tetrahedron* **2014**, *70*, 5999–6011; (b) Hu, T. S.; Lin, K. T.; Mu, C. C.; Kuo, H. M.; Chen, M. C.; Lai, C. K. *Tetrahedron* **2014**, *69*, 9204–9213; (c) Lin, K. T.; Kuo, H. M.; Sheu, H. S.; Lai, C. K. *Tetrahedron* **2013**, *69*, 9045–9055; (d) Kuo, H. M.; Li, S. Y.; Sheu, H. S.; Lai, C. K. *Tetrahedron* **2012**, *68*, 7331–7337; (e) Liao, C. T.; Wang, Y. J.; Huang, C. S.; Sheu, H. S.; Lee, G. H.; Lai, C. K. *Tetrahedron* **2007**, *63*, 12437–12445.
6. (a) Reddy, M. K.; Varathan, E.; Lobo, N. P.; Das, B. B.; Narasimhaswamy, T.; Ramanathan, K. V. *J. Phys. Chem. C* **2014**, *118*, 15044–15053; (b) Romiszewski, J.; Tokarove, Z. R.; Mieczkowski, J.; Gorecka, E. *New J. Chem.* **2014**, *38*, 2927–2934; (c) Gao, H.; Ye, Y.; Kong, L.; Cheng, X.; Prehm, M.; Ebert, H.; Tschierski, C. *Soft Mater.* **2012**, *8*, 10921–10931; (d) Matharu, A. S.; Karadakov, P. B.; Cowling, S. J.; Hegde, G.; Komitov, L. *Liq. Cryst.* **2011**, *38*, 207–232; (e) Seed, A. *Chem. Soc. Rev.* **2007**, *36*, 2046–2069; (f) Parasko, A. J.; Swager, T. M. *Chem. Mater.* **2002**, *14*, 4543–4549; (g) Eichhorn, S. H.; Paraskos, A. J.; Kishikawa, K.; Swager, T. M. *J. Am. Chem. Soc.* **2002**, *43*, 12742–12751.
7. Lin, H. Y.; Kuo, H. M.; Wen, S. G.; Sheu, H. S.; Lee, G. H.; Lai, C. K. *Tetrahedron* **2012**, *68*, 6231–6239.
8. (a) Han, J. J. *Mater. Chem. C* **2013**, *1*, 7779–7797; (b) Zhang, P.; Qu, S.; Wang, H.; Bai, B.; Li, M. *Liq. Cryst.* **2008**, *35*, 389–394; (c) Wang, H.; Zhang, F.; Bai, B.; Zhang, P.; Shi, J.; Yu, D.; Zhao, Y.; Wang, Y.; Li, M. *Liq. Cryst.* **2008**, *35*, 905–912; (d) Chai, C.; Yang, Q.; Fan, X.; Chen, X.; Shen, Z.; Zhou, Q. *Liq. Cryst.* **2008**, *35*, 133–141; (e) Zhang, X. B.; Tang, B. C.; Zhang, P.; Li, M.; Tian, W. J. *J. Mol. Struct.* **2007**, *846*, 55–64.
9. (a) Qu, S.; Wang, L.; Liu, X.; Li, M. *Chem.—Eur. J.* **2011**, *17*, 3512–3518; (b) Zhang, P.; Bai, B.; Wang, H.; Qu, S.; Yu, Z.; Ran, X.; Li, M. *Liq. Cryst.* **2009**, *36*, 7–12; (c) Qu, S.; Li, M. *Tetrahedron* **2007**, *63*, 12429–12436.
10. (a) Tomi, I. H. R. *J. Saudi Chem. Soc.* **2012**, *16*, 153–159; (b) Cristiano, R.; Ely, F.; Gallardo, H. *Liq. Cryst.* **2005**, *32*, 15–25.
11. (a) Barbera, J.; Godoy, M. A.; Hidalgo, P. I.; Parra, M. L.; Ulloa, J. A.; Vergara, J. M. *Liq. Cryst.* **2011**, *38*, 679–688; (b) Yelamaggad, C. V.; Achalkumar, A. S.; Rao, D. S. S.; Prasad, S. K. *J. Org. Chem.* **2009**, *74*, 3168–3171; (c) Kim, B. G.; Kim, S.; Park, S. Y. *Tetrahedron Lett.* **2001**, *42*, 2697–2699.
12. (a) Gallardo, H.; Ferreira, M.; Vieira, A. A.; Westphal, E.; Molin, F.; Echer, J.; Bechtold, I. H. *Tetrahedron* **2011**, *67*, 9491–9499; (b) Torgova, S. I.; Geivandova, T. A.; Francescangeli, O.; Striazzi, A. *Ind. Acad. Sci.* **2003**, *61*, 239–248.
13. Wang, C.; Palsson, L. O.; Batsanov, A. S.; Bryce, M. R. *J. Am. Chem. Soc.* **2006**, *128*, 3789–3799.